Feature Article

Exploring Potential Energy Surfaces for Chemical Reactions: An Overview of Some Practical Methods

H. BERNHARD SCHLEGEL
Department of Chemistry, Wayne State University, Detroit, Michigan 48202

Received 25 July 2002; Accepted 4 November 2002

Abstract: Potential energy surfaces form a central concept in the application of electronic structure methods to the study of molecular structures, properties, and reactivities. Recent advances in tools for exploring potential energy surfaces are surveyed. Methods for geometry optimization of equilibrium structures, searching for transition states, following reaction paths and *ab initio* molecular dynamics are discussed. For geometry optimization, topics include methods for large molecules, QM/MM calculations, and simultaneous optimization of the wave function and the geometry. Path optimization methods and dynamics based techniques for transition state searching and reaction path following are outlined. Developments in the calculation of *ab initio* classical trajectories in the Born-Oppenheimer and Car-Parrinello approaches are described.

 J Comput Chem 24: 1514–1527, 2003

Key words: potential energy surface; geometry optimization; *ab initio* molecular dynamics; transition states; reaction paths

Introduction

From a computational point of view, many aspects of chemistry can be reduced to questions about potential energy surfaces (PES). A model surface of the energy as a function of the molecular geometry is shown in Figure 1 to illustrate some of the features. One can think of it as a hilly landscape, with valleys, mountain passes and peaks. Molecular structures correspond to the positions of the minima in the valleys on a potential energy surface. The energetics of reactions are easily calculated from the energies or altitudes of the minima for reactants and products. Reaction rates can be obtained from the height and profile of the mountain pass separating the valleys of the reactants and products. The shape of the valley around a minimum determines the vibrational spectrum. Each electronic state of a molecule has a separate potential energy surface, and the separation between these surfaces yields the electronic spectrum. Properties of molecules such as dipole moment, polarizability, NMR shielding, etc., depend on the response of the energy to applied electric and magnetic fields. Thus, the structure, properties, reactivity, and spectra of molecules can be readily understood in terms of potential energy surfaces. Except in very simple cases, the potential energy surface cannot be obtained from experiment. However, the field of computational chemistry has developed a wide array of methods for exploring potential energy surface.

A potential energy surface arises naturally when the Born–Oppenheimer approximation is invoked in the solution of the Schrödinger equation for a molecular system. Essentially, this assumes that the electronic distribution of the molecule adjusts quickly to any movement of the nuclei. Except when potential energy surfaces for different states get too close to each other or cross, the Born–Oppenheimer approximation is usually quite good. Thus, the energy and behavior of a molecule can be expressed as a function of the positions of the nuclei, that is, a potential energy surface. The task for computational chemistry is to explore this potential energy surface with methods that are efficient and accurate enough to describe the chemistry of interest.

"Tools for Exploring Potential Energy Surfaces" was the topic of a recent ACS symposium organized by the author.[1] The present article provides an overview of some recent developments in this area, highlighting a few of our own contributions to the Gaussian series of programs.[2] The focus is on potential energy surfaces obtained by quantum chemical methods, because our interest is in reactive systems. Such calculations tend to require considerable computer resources, but with continuing advances in software and hardware, they can be applied to rather sizeable systems with quite respectable accuracy.[3–6] Molecular mechanics calculations are much cheaper, and have long been used to address questions of structure and dynamics,[5–7] but the types of reactions that can be treated by molecular mechanics is rather limited. However, QM/MM techniques that combine quantum mechanics (QM) for the reactive region and molecular mechanics (MM) for the remain-

Correspondence to: H. B. Schlegel

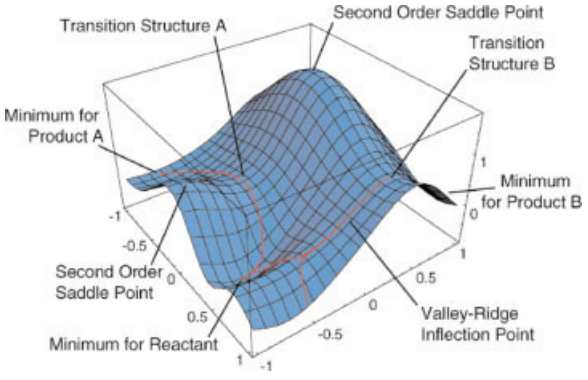

Figure 1. Model potential energy surface showing minima, transition states, a second-order saddle point, reaction paths, and a valley ridge inflection point (from ref. 26 with permission from World Scientific Publishing).

der are very promising, especially for biochemical systems.[8–18] The dynamics of molecules moving on potential energy surfaces[19–24] have traditionally been calculated using analytic potential energy surfaces obtained by fitting to experimental and computational data. Because of improvements in software and hardware, molecular dynamics of modest size systems can now be explored using direct methods (for a review, see ref. 25). In this approach, often termed *ab initio* molecular dynamics (AIMD), electronic structure methods are used to calculate the potential energy and its derivatives "on the fly," as they are needed for the integration of the equations of motion of the system.

Topics considered in the present overview include geometry optimization of equilibrium structures, searching for transition states, following reaction paths and *ab initio* molecular dynamics. Methods for geometry optimization of minima and transition states have a long history and are discussed in a number of reviews.[26–30] Some recent developments include methods for large molecules,[31–39] special techniques for QM/MM calculations,[40–43] and simultaneous optimization of the wave function and the geometry.[44–47] Global optimization, conformational searching, etc., are outside the scope of this article; discussions of these topics can be found elsewhere.[48–52] Once the appropriate structures on the potential energy surface have been optimized, a reaction mechanism can be mapped out by finding the lowest energy reaction path that connects the reactants to the products via suitable transition states and intermediates.[53–56] New techniques in this area include path optimization methods[57–64] and dynamics-based methods.[65–68] Reaction path information can also be used to calculate reaction rates by variational transition state theory and reaction path Hamiltonian methods,[70–74] but the details cannot be cover in this brief overview. Steepest descent reaction paths are only a crude approximation to the motion of a molecule across a potential energy surface. The classical trajectories of a molecule moving on a potential energy surface explore a wider region than are traced out by the reaction path.[19–24] The calculation of classical trajectories by *ab initio* molecular dynamics methods is a comparatively new area[25] and is expanding rapidly as affordability of computer power increases and more efficient software is developed. Quantum dynamics on potential energy surfaces is outside the scope of the present article.[75–77] The intent of this article is not to provide a thorough review of these fields, but only to provide highlights of some recent developments in practical methods for exploring potential energy surfaces.

Optimizing Equilibrium Geometries

In any optimization problem, the choice of coordinates can have an important influence on the efficiency of the optimization. Cartesian coordinates provide a simple and unambiguous representation for molecular geometries, and are used for calculating the molecular energy and its derivatives. However, the potential energy surface has very strong coupling between coordinates when represented in Cartesians. Bond lengths, valence angles, and torsions about bonds are more appropriate coordinates to describe the behavior of molecules. Because they express the natural connectivity of chemical structures, there is much less coupling between these internal coordinates. For cyclic molecules, there are more bonds, angles and dihedrals than the three $N_{\text{atoms}} - 6$ internal degrees of freedom, and the coordinate system has some redundancy. There are a number of different flavors of redundant internal coordinate systems (primitive, natural, delocalized),[78–83] and all work better than Cartesians or nonredundant internals (e.g., Z-matrix coordinates), especially for polycyclic systems. The transformation of Cartesian coordinates and displacements to internals is straightforward, but the transformation of the gradients (and Hessian, if necessary) requires a generalized inverse of the transformation matrix.[78]

$$\Delta\mathbf{q} = \mathbf{B}\Delta\mathbf{x}, \quad \mathbf{g}_q = \mathbf{B}^{-1}\mathbf{g}_x, \quad \mathbf{H}_q = \mathbf{B}^{-T}(\mathbf{H}_x - \partial\mathbf{B}/\partial\mathbf{x}\,\mathbf{g}_q)\mathbf{B}^{-1} \quad (1)$$

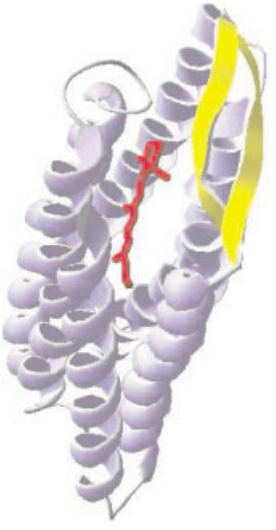

Figure 2. Schematic for a QM/MM calculation of bacteriorhodopsin (ONIOM(PM3:Amber) calculation, with α helices (show in *ribbon* format) calculated with the Amber force field, and the retinal chromophore (shown in *tube* format) calculated at the PM3 level) (adapted from ref. 43 with permission).

where $\mathbf{x}$ are the Cartesian coordinates, $\mathbf{q}$ are the (redundant) internal coordinates, $\mathbf{B} = \partial\mathbf{q}/\partial\mathbf{x}$ is the Wilson B matrix[84] and $\mathbf{g}_x = dE/d\mathbf{x}$ is the Cartesian gradient, and $\mathbf{H}_x = d^2E/d\mathbf{x}^2$ is the Cartesian Hessian. Because of the redundancy and the curvilinear nature of the internal coordinates, the transformation back to Cartesians involves an iterative process as well as a generalized inverse.[78] The calculation of a generalized inverse scales as $O(N^3)$, where N is the number of atoms or the number of redundant internals. For small molecules, this is not a problem. However, for larger systems or inexpensive levels of theory, these transformations can become a bottleneck. In recent years, a number of methods have been developed to overcome these difficulties,[31–39] using techniques such as iterative solutions to linear equations, Cholesky decomposition and sparse matrix methods. For electronic structure calculations, the extra work required to transform to internal coordinates for the optimization is more than compensated by the reduced number of steps required to reach the minimum. Even for molecular mechanics calculations (and the MM part of QM/MM calculations), the trade-off may be favorable in some circumstances.

For optimization of molecular geometries, it is well established[26–30] that quasi-Newton methods[85–88] are one of the best approaches. The displacement toward the minimum is given by

$$\Delta\mathbf{q} = -\mathbf{H}^{-1}\mathbf{g} \tag{2}$$

The Hessian is not usually calculated explicitly, but is obtained by updating an initial estimate. Suitable estimates of the Hessian can be readily obtained from empirical estimates,[46,89,90] molecular mechanics or semiempirical methods. The Broyden–Fletcher–Goldfarb–Shanno (BFGS) formula[91–94] is acknowledged as one of the best updating schemes.

$$\mathbf{H}^{\text{new}} = \mathbf{H}^{\text{old}} + \Delta\mathbf{H}^{\text{BFGS}} \tag{3}$$

$$\Delta\mathbf{H}^{\text{BFGS}} = \Delta\mathbf{g}\Delta\mathbf{g}^T/\Delta\mathbf{x}^T\Delta\mathbf{g} - \mathbf{H}^{\text{old}}\Delta\mathbf{x}\Delta\mathbf{x}^T\mathbf{H}^{\text{old}}/\Delta\mathbf{x}^T\mathbf{H}^{\text{old}}\Delta\mathbf{x} \tag{4}$$

We have found that a modification of Bofill's update[95] for transition states is very useful for minima,

$$\Delta\mathbf{H} = \phi\Delta\mathbf{H}^{\text{BFGS}} + (1-\phi)\Delta\mathbf{H}^{\text{MS}},$$

$$\phi = |\Delta\mathbf{x}^T(\Delta\mathbf{g} - \mathbf{H}^{\text{old}}\Delta\mathbf{x})|/|\Delta\mathbf{x}|\,|\Delta\mathbf{g} - \mathbf{H}^{\text{old}}\Delta\mathbf{x}| \tag{5}$$

$$\Delta\mathbf{H}^{\text{MS}} = (\Delta\mathbf{g} - \mathbf{H}^{\text{old}}\Delta\mathbf{x})(\Delta\mathbf{g} - \mathbf{H}^{\text{old}}\Delta\mathbf{x})^T/\Delta\mathbf{x}^T(\Delta\mathbf{g} - \mathbf{H}^{\text{old}}\Delta\mathbf{x}) \tag{6}$$

which combines BFGS with the Murtagh-Sargent (MS) symmetric rank 1 update. For very large systems, storage of the full Hessian is impractical, and methods such as limited memory BFGS (LBFGS) are useful.[46,96–104] These store a diagonal Hessian and vectors to perform a limited series of updates (this requires only O(N) cpu and storage).

In determining the displacement toward the minimum, the Newton step needs to be controlled in some fashion.[85–88] If some of the eigenvalues of the Hessian are small or are negative, the step will be too large or in the wrong direction. Rational function optimization (RFO), trust radius method (TRM), and their variants are quite satisfactory for controlling the step size,[95,105–109] for example:

$$\Delta\mathbf{q} = -(\mathbf{H} + \lambda\mathbf{I})^{-1}\mathbf{g} \tag{7}$$

where λ is chosen so that the step is in the descent direction and of appropriate length. These are normally computed using the eigenvalues and eigenvectors of the Hessian [an $O(N^3)$ computational task]. For larger systems, where this becomes a bottleneck, we have developed an $O(N^2)$ iterative method that avoids the costly diagonalization.[32] To handle situations where the potential energy surface is anharmonic, it is desirable to include a line search. A simple interpolation using a cubic or quartic polynomial will often suffice (and does not require additional energy calculations).[85,86,110]

Another optimization method that is very efficient, especially in the vicinity of the minima, is the GDIIS approach.[33,111,112] The technique is based on a linear interpolation/extrapolation of the available structures so as to minimize the length of an error vector.

$$\mathbf{q}^* = \sum c_i\mathbf{q}_i, \quad \sum c_i = 1 \tag{8}$$

A simple Newton step or the gradient can be used as the error vector.

$$\mathbf{e}_i = -\mathbf{H}^{-1}\mathbf{g}_i \quad \text{or} \quad \mathbf{e}_i = \mathbf{g}_i, \quad \mathbf{r} = \sum c_i\mathbf{e}_i \tag{9}$$

The minimization of the $|\mathbf{r}|^2$ leads to a least-squares problem that can be solved for the coefficients, c_i. The next point in the optimization is given by:

$$\mathbf{q}^{\text{new}} = \sum c_i(\mathbf{q}_i - \mathbf{H}^{-1}\mathbf{g}_i) \tag{10}$$

Farther from the minimum, the GDIIS method may misbehave, converging to a nearby critical point of higher order, or oscillating about an inflection point. A number of improvements have been implemented to overcome these difficulties.[33,112] The problem of converging to a higher order critical point can be controlled by comparing the GDIIS step with a reference step, for example, a quasi-Newton step using the RFO or trust radius method. If the angle between the GDIIS step and the reference step is greater than a threshold, the reference step is taken instead. Limits are also placed on the length of the GDIIS step compared to the reference, and on the magnitude of the coefficients. With suitable updating of the Hessian [i.e., eq (3) or (5)], the performance of the controlled GDIIS method is equal to or better than the quasi-Newton RFO method. If a diagonal Hessian is used and a limited number of error vectors is retained, the computational effort and memory requirements of the GDIIS method scale linearly with the size of the system.

For large systems, hybrid energy methods such as QM/MM[8–18] and ONIOM,[10,113–115] that combine different levels of theory into one calculation, can be very useful. A higher level of theory is used to model the smaller, chemically important region and a lower level of theory is used for the larger environment, as illustrated in Figure 2. Covalent bonds that cross the boundary between the two regions can be treated by using link atom or hybrid orbitals.

Geometry optimization methods can take advantage of the fact that a large region is treated by inexpensive molecular mechanics while only a small part requires expensive quantum mechanical calculations. It is common to employ a series of microiterations to fully optimize the MM region for each optimization step in the QM region.[40–43] However, some problems can arise when separated optimizers are used for the QM and the MM regions. In particular, geometrical constraints applied to the MM region, can make the uncoupled optimizations of the MM and QM regions very slow to converge. In our approach,[43] we choose the internal coordinates of the QM region so that they remain constant during the microiterations of the MM region. The Cartesian coordinates used for the MM region are augmented to permit rigid body translation and rotation of the QM region. This is essential if any atoms in the MM region are constrained, but also improves the efficiency of unconstrained optimizations. Because of the microiterations, special care is also needed for the optimization step in the QM region so that the system remains in the same local valley during the course of the optimization.[43]

Many electronic structure calculations can be phrased in terms of minimizations of the variational energy with respect to variables in the wavefunction. Algorithms such as DIIS, conjugate gradient, and Newton-Raphson methods have been used to converge Hartree–Fock and density functional calculations.[44–46,116–122] Because this problem is similar to optimization of geometry, one can contemplate optimizing the geometry and the wave function simultaneously.[44–46] This would avoid the tedious convergence of the wave function for each step in the optimization. Even the simple trick of reducing the SCF convergence criteria when the structure is far from the minimum can save as much as 30% of the cpu time.[123] In the second-order approach to simultaneous optimization of the geometry and the wave function, the gradients and Hessians are calculated with respect to the nuclear positions and the molecular orbital coefficients.[45] The RFO method is used to control the Newton step toward the minimum. In the first-order approach, the nuclear and wave function gradients are used in a quasi-Newton minimization algorithm.[44,46] Both of these approaches are competitive with conventional geometry optimization using converged wavefunctions. However, neither has seen widespread use. Recently, we have implemented a first-order simultaneous optimization using the DIIS method for minimizing the energy with respect to both the electronic structure and the geometry.[47] Preliminary indications are that this conceptually simple approach is efficient and robust.

Another task that can be cast in terms of a minimization is the search for conical intersections and avoided crossing.[124–127] Two potential energy surfaces representing different electronic states can cross if they are of different symmetry (spatial or spin). If they are the same symmetry, the crossing is avoided, except where the coupling matrix element (in a diabatic picture) is zero. The seam of intersection has a dimension of $3\,N_{\text{atoms}} - 8$ or $3\,N_{\text{atoms}} - 7$, depending on whether or not the surfaces are the same symmetry. We wish to find the lowest point of intersection, which can be a minimization task with many degrees of freedom. This can be done with the aid of Lagrangian multipliers to constrain the energies for the two surfaces to be equal.[127–129] Alternatively, projection methods can be used to treat these constraints. Using this approach, we minimize the square of the energy difference in the one or two dimensional space of the intersection and minimizes the energy of the upper surface in the remaining $3\,N_{\text{atoms}} - 8$, or $3\,N_{\text{atoms}} - 7$ dimensions.[130]

$$\tilde{\mathbf{g}} = d(E_2 - E_1)^2/d\mathbf{x} + (\mathbf{1} - \mathbf{v}_1\mathbf{v}_1^T/|\mathbf{v}_1|^2)(\mathbf{1} - \mathbf{v}_2\mathbf{v}_2^T/|\mathbf{v}_2|^2)dE_2/d\mathbf{x} \quad (11)$$

where $\mathbf{v}_1 = d(E_2 - E_1)/d\mathbf{x}$ and $\mathbf{v}_2 = \mathrm{d}H_{12}/d\mathbf{x}$. Because the square of the energy difference is better behaved than the absolute value of the difference, the corresponding gradient can be used without further modification or constraint in a conventional quasi-Newton optimization algorithm.

Finding Transition States

A transition state is a stationary point on a potential energy surface that corresponds to a mountain pass (see Fig. 1). It is a maximum in one and only one direction (along the transition vector, going from one valley to another) and a minimum in all other perpendicular directions (three $N_{\text{atoms}} - 7$ degrees of freedom). Transition states are often more difficult to find, and many algorithms have been developed to search for them (see refs. 26, 27, 29, and 30 for some reviews). In principle, a transition state could be found by minimizing the norm of the gradient,[131–134] but this is usually not a good idea. Provided that the initial structure is close enough to the quadratic region of the transition state, the quasi-Newton[85–88] and GDIIS[33,111,112] methods for minimization can be adapted to find transition states. The initial Hessian must have the correct number of negative eigenvalues (one and only one), and the corresponding eigenvector must be a suitable approximation to the transition vector (i.e., pointing from one valley to the other). During the course of the optimization, the Hessian must be updated. The BFGS formula is not acceptable, because the update is positive definite. Powell-symmetric-Broyden (PSB) and symmetric rank 1 (Murtagh–Sargent, MS) do not force a positive definite update,[85–88] and are more appropriate for transition states. Bofill[95,103,135–138] developed a hybrid update that is superior to both of these

$$\Delta\mathbf{H}^{\text{Bofill}} = \phi\Delta\mathbf{H}^{\text{PSB}} + (1 - \phi)\Delta\mathbf{H}^{\text{MS}},$$
$$\phi = |\Delta\mathbf{x}^T(\Delta\mathbf{g} - \mathbf{H}^{\text{old}}\Delta\mathbf{x})|^2/|\Delta\mathbf{x}|^2|\Delta\mathbf{g} - \mathbf{H}^{\text{old}}\Delta\mathbf{x}|^2 \quad (12)$$

$$\Delta\mathbf{H}^{\text{BSP}} = [(\Delta\mathbf{g} - \mathbf{H}^{\text{old}}\Delta\mathbf{x})^T\Delta\mathbf{x} + \Delta\mathbf{x}^T(\Delta\mathbf{g} - \mathbf{H}^{\text{old}}\Delta\mathbf{x})]/\Delta\mathbf{x}^T\Delta\mathbf{x}$$
$$- [(\Delta\mathbf{g} - \mathbf{H}^{\text{old}}\Delta\mathbf{x})^T\Delta\mathbf{x}]\Delta\mathbf{x}\Delta\mathbf{x}^T/(\Delta\mathbf{x}^T\Delta\mathbf{x})^2 \quad (13)$$

Bofill also observed that for larger systems, the energy needs to be minimized with respect to most of the coordinates whereas only a few coordinates are involved in the transition vector.[103,104,138,139] Because these coordinates can be readily identified by comparing the reactants and products, the Bofill update can be used for the small Hessian update pertaining to them. The remaining coordinates form a much larger space and can be treated with the BFGS update.

The major problem in optimizing transition states is to get near enough to the quadratic region. Quite a number of methods have been developed to get close to transition states. Because these have

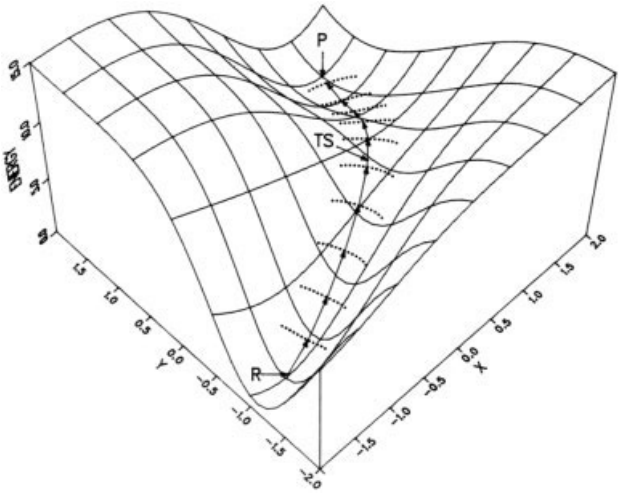

Figure 3. The walking up valleys approach to optimizing transition states (from ref. 267 with permission).

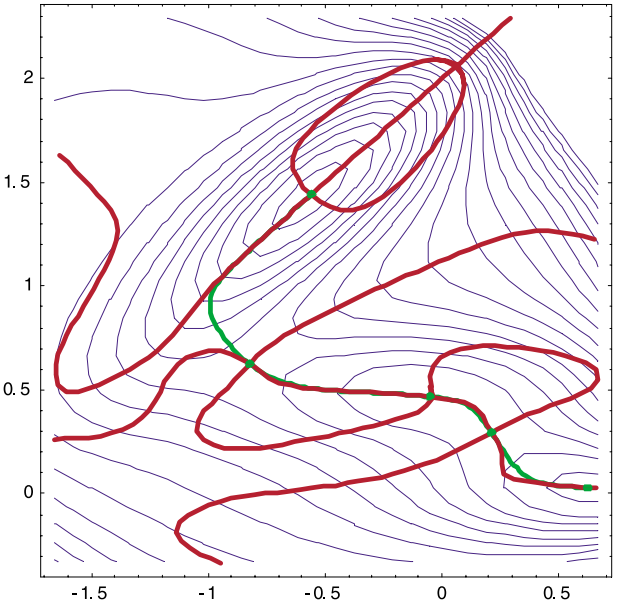

Figure 4. Gradient extremals (red) and steepest descent reaction paths (green) on the Müller–Brown surface.

been reviewed elsewhere,[26,27,29,30] only some generalities and a few specifics will be considered here. One approach is to approximate the potential energy surface for a reaction as the intersection surfaces for the reactants and products, modeled by molecular mechanics or valence bond methods.[140–143] The lowest point on the seam of intersection can yield good estimates of the transition state geometry and Hessian (but molecular mechanics force fields may have to be modified to handle the larger distortions from equilibrium). A more general alternative is the coordinate driving or distinguished coordinate method (i.e., stepping a chosen variable and optimizing the remaining ones). In favorable circumstances, this approach can be used to climb from reactants or products to the transition state, but it can run into difficulties such as discontinuities if the reaction path is strongly curved.[144–146] The reduced gradient following method is an improvement on this approach, and is better able to handle curved reaction paths.[147–152] Walking up valleys[105,153–157] or following the shallowest ascent path[158] is a better strategy, as shown in Figure 3. In this method, a step is taken uphill along the eigenvector with the lowest eigenvalue, and downhill along all the other directions. Similar to the RFO and trust radius methods, the step is controlled by adding an offset to the Hessian, as in eq. (7). The parameter λ is chosen so that $\mathbf{H} + \lambda \mathbf{I}$ has only one negative eigenvalue and so that the Newton step with the offset Hessian has the appropriate length. Sometimes different λs are used for the ascent and descent portions of the step.[106,107,157] These approaches greatly expand the radius of convergence of transition state optimizations, provided that the initial Hessian is chosen so that it possesses an eigenvector in a suitable ascent direction.[143] A serious problem with "walking up valleys" is that only transition states at the end of the valley can be found by this approach. However, many interesting transition states are to the side of the valley floor and cannot be found by this method.

An alternative to "walking up valleys" is following gradient extremals.[158–160] Along a gradient extremal curve, the derivative of the gradient norm is zero subject to the constraint that the energy is constant. Equivalently, the gradient is an eigenvector of the Hessian on a gradient extremal curve. A number of algorithms for following gradient extremals have been developed.[161–163] Because gradient extremals are locally defined and pass through all stationary points, they can be followed from minima to transition states (whereas steepest descent paths cannot be followed uphill to transition states). However, considerable care is needed, because gradient extremals do not necessarily connect stationary points as directly as steepest descent reaction paths, as illustrated in Figure 4. In fact, Bondensgard and Jensen[164] have demonstrated that the behavior of gradient extremals is much too complicated to be practical even for molecules as simple as formaldehyde.

Synchronous transit methods start from the reactant and product, and find the maximum along a linear or quadratic path across

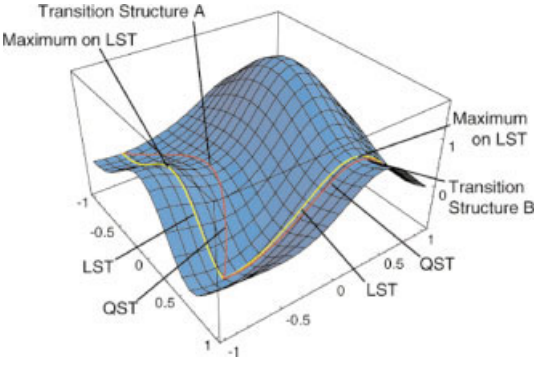

Figure 5. Linear synchronous transit (LST) paths (yellow) and quadratic synchronous transit (QST) paths (red) on a model potential energy surface (from ref. 26 with permission from World Scientific Publishing).

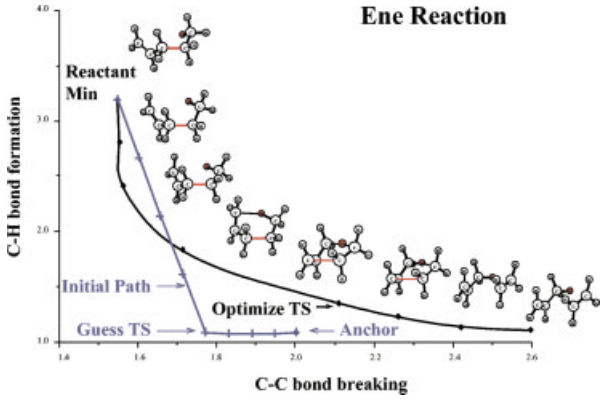

Figure 6. Reaction path optimization for the ene reaction $C_5H_{10} \rightarrow C_3H_6 + C_2H_4$ (from ref. 62 with permission).

the surface (see Fig. 5).[165] Often this provides a structure close enough to the transition state for quasi-Newton or shallowest ascent methods to succeed. This idea can be generalized such that two structures instead of one are used to start a transition state search. We have used two structures—one in the reactant valley, and the other in the product valley—to specify an approximate reaction path and bracket the transition state.[166] Updating the Hessian while searching uphill along the path ensures that the Hessian has a negative eigenvalue. The approximate path is then used to control the quasi-Newton/shallowest ascent search for the transition state.

The saddle method[167–169] also starts with two points—one on the reactant side of the transition state, and the other on the product side. The lowest energy point is stepped toward the other and optimized with the constraint that the distance between them is fixed. As the two points converge toward each other, they provided better bounds on the transition state. Ridge following extends the idea of bracketing the transition state.[170,171] Two structures, one on either side of the ridge separating the reactant and product valleys, are stepped toward each other to more tightly bracket the ridge, and are moved parallel to the ridge to find its lowest point ridge, i.e., the transition state.

This idea can be generalized to optimize not only two points, but the entire path between reactants and products.[57–64] Points are equally spaced along an approximate reaction path. The points are then moved so that they minimize the barrier and approximate the reaction path. This can be accomplished by minimizing the integral of the energy along the path.

$$I = 1/L \int E(s)ds = 1/2L \sum [E(\mathbf{x}_{i+1}) + E(\mathbf{x}_i)]|\mathbf{x}_{i+1} - \mathbf{x}_i| \quad (14)$$

where $L = \Sigma\, |\mathbf{x}_{i+1} - \mathbf{x}_i|$ is the length of the path. Additional forces are added to keep the points equally spaced and to prevent the path from becoming kinked.[57–61] This has given rise to the name "nudged elastic band" for this method of optimization. However, the efficiency of these methods[61] is still relatively poor compared to some of the methods discussed above. As an alternative, we developed a method for optimization of the path in which one point optimizes to the transition state and other points optimize to the steepest descent path, as shown in Figure 6.[62] Other variants of this concept include the chain[69] and locally updated plane[63] methods. The conjugate peak refinement method[64] is a dynamic version of the chain method, where points are added or deleted as a result of optimizations in directions conjugate to the current path.

Optimizing a large number of points along a reaction path can be expensive. However, the thought of beginning a transition state optimization from the reactant and product minima is appealing. We are developing a method in which a point in the reactant valley and another in the product valley attracted to each other and move toward a transition state in a pseudotrajectory (see Fig. 7). As they approach each other, the steps are adjusted so that they stay on opposite sides of the ridge and follow it down to the transition state.

In some cases, the product of a reaction may not be known beforehand. For example, one may be interested in the lowest energy pathway for a rearrangement or decomposition of a given reactant. In terms of the landscape of a potential energy surface, one can imagine gradually filling a valley with water, and finding when and where it overflows. Irikura[172] has developed an algorithm that follows an iso-potential contour on a energy surface until it finds a transition state. Although rather time consuming, this has lead to some surprising reaction mechanisms in a number of cases. In another approach, coordinate driving with in a selected subset of the coordinate system has been used to automatically explore a reaction network in a systematic fashion.[173] A third approach uses molecular dynamics on a modified potential to simulate unimolecular decomposition.[174] However, rather long simulations may be required.

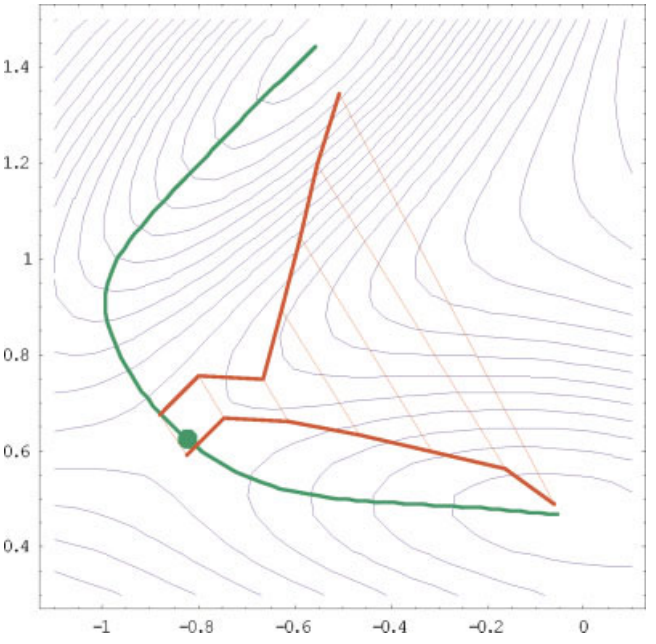

Figure 7. Bracketing the transition state starting from a point in the reactant valley and another in the product valley attracted to each other and move toward a transition state in a pseudotrajectory.

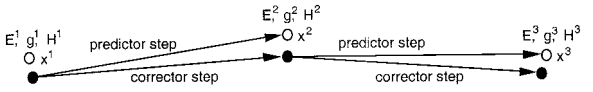

Figure 8. Hessian-based predictor-corrector algorithm for integrating classical trajectories (from ref. 187 with permission).

Following Reaction Paths

After a transition state has been located and a frequency calculation has verified that it has one and only one imaginary frequency, it is often necessary to confirm that it connects the desired reactants and products. The reaction path is also needed for calculating reaction rates by variational transition state theory or reaction path Hamiltonian methods.[70–74] These provide more accurate treatments of reaction rates than simple transition state theory.

The steepest descent reaction path is defined by

$$d\mathbf{x}(s)/ds = -\mathbf{g}(s)/|\mathbf{g}(s)| \quad (15)$$

If mass weighted coordinates are used, the steepest descent path is the intrinsic reaction coordinate.[175] Methods for following the reaction path from the transition state down to the reactants and down to the products have been reviewed in a number of articles.[53–56] One of the first practical techniques was the Ishida–Morokuma–Komornicki method,[176] a stabilized form of the Euler method for integrating differential equations. Page and McIver[56,177,178] developed a series of methods for integrating eq. (15) based on a local quadratic approximation (LQA) to the potential energy surface, and corrections based on higher order Taylor expansions. Other numerical methods for integrating ordinary differential equations can also be used to follow the path.[179–181] However, the differential equations for steepest descent paths tend to be stiff; small step sizes, and special methods may be needed.[182] Implicit methods for integrating differential equations can use larger step sizes to follow the reaction path, but at the cost of an optimization at each step. The Müller–Brown approach[167] is an implicit Euler method. The second-order GS technique that we developed a number of years ago corresponds to an implicit trapezoid method.[183,184] We have also extended these ideas to higher implicit methods.[185]

Direct classical trajectory methods (see below) can be adapted to follow reaction paths.[65–68] We have developed some improved techniques to control the accuracy of reaction path following using a damped velocity Verlet method.[68] For larger molecules, this approach can be significantly more efficient than the conventional method for following reaction paths. We have also adapted[69] our Hessian-based predicitor-corrector method for integrating classical trajectories[186–188] (see below and Fig. 8) to produce an algorithm for following reaction paths and calculating projected frequencies along the path[189] that closely resembles our fourth-order implicit method.[185]

The previous section described methods for finding transition states by optimizing a set of points on the reaction path.[30,57–60,62–64] By design, these methods also yield a representation of the reaction path. An extension of this approach, the replica path method, computes not only the path but also the free energy along the path.[190] A molecular dynamics simulation for motion perpendicular to the path provides an estimate of the free energy for each point along the path. Slow growth molecular dynamics simulations have been employed to estimate the free energy along a predetermined reaction path.[191] Free energy perturbation methods have also been used to obtain the free energy along a coordinate driving path.[40] An alternative approach obtains reaction paths and rates by using Monte Carlo method to sample an ensemble of transition paths.[192–196] Yet another approach obtains free energy profiles along reaction paths by an adiabatic separation between the reaction coordinate and the remaining degrees of freedom.[197,198] This is achieved by assigning an artificial large mass and high temperature to the reaction coordinate.

Ab Initio *Molecular Dynamics (AIMD)*

Classical trajectory calculations[20–24] provide greater insight into the dynamics of reactions than can be obtained from variational transition state theory and reaction path Hamiltonian methods.[70–74] Molecular dynamics calculations may involve extensive sampling of initial conditions and/or long simulation times. Typically, trajectory calculations have been carried out using global, analytical potential energy surfaces, so that the energy and its derivatives can be calculated rapidly whenever needed during the integration of the equations of motion. Potential energy surfaces obtained from well parameterized molecular mechanics calculations can be quite satisfactory for simulations near equilibrium. However, for reactive systems, specific potential energy surfaces must be devised for each unique system. Constructing potential energy surfaces by fitting to experimental data and/or *ab initio* molecular orbital energies can be both tedious and full of pitfalls.[199,200] Because of advances in computer speed and molecular orbital software, it has become possible to use *ab initio* and semiempirical molecular orbital calculations directly in classical trajectory calculations and thus avoid the fitting process.[25]

There are a number of aspects to molecular dynamics simulations. First is the choice of the initial conditions.[201] Enough trajectories must be calculated, or a single trajectory must be run for a long enough time to get statistically significant results. Then, for each trajectory, the initial coordinates and velocities need to be chosen so that they sample an ensemble that is suitable for the system being simulated (e.g., microcanonical, thermal, etc.). Second, the appropriate equations of motion need to be integrated (e.g., classical or quantum, with or without Nosé–Hoover thermostat chains to control temperature, with or without Langevin pistons to control pressure, etc.). Finally, the results must be analyzed[202] (e.g., reaction rates, branching ratios, energy partitioning, etc., for reactive systems; free energies, entropies, potentials of mean force, autocorrelation functions, etc., for free energy simulations, etc.). These and many other topics are discussed in chapters and monographs on molecular dynamics.[19–24,203–212] The aspect most relevant to the present overview on exploring potential energy surfaces is the efficient and accurate integration of the equations of motion using direct methods that evaluate the electronic structure "on the fly."

Direct classical trajectory calculations can be grouped into two major categories: Born–Oppenheimer (BO) methods, and Car–

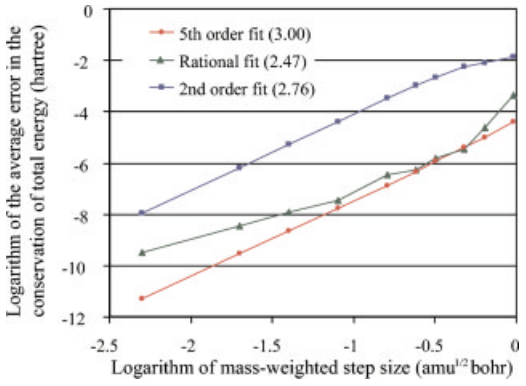

Figure 9. Comparison of the error in the conservation of energy vs. step size for trajectories integrated with the second-order Hessian-based method (blue) and the Hessian-based predictor-corrector method with a fifth-order polynomial (red) or a rational function (green) for the corrector step (slopes of the least squares fits in parenthesis).

Parrinello (CP) methods.[25] For the former, each time that information about the potential energy surface is needed for a given nuclei configuration, the electronic structure calculation is fully converged. This yields the energy and its derivatives in the Born–Oppenheimer approximation, which are then used in the numerical integration of the equations of motion for the nuclei. In the Car–Parrinello approach,[213] an extended Lagrangian is used to propagate the wave function as well as the nuclei. With an appropriate adjustment of the time scales for the propagation of the wavefunction, both can be propagated satisfactorily, without the extra work of converging the wave function at each step. The resulting dynamics of the nuclei are comparable to that obtained with the Born–Oppenheimer approximation.

Born–Oppenheimer Methods

The most straightforward technique for direct Born–Oppenheimer dynamics uses only the energy and gradient calculated by electronic structure methods. This can be achieved by linking an electronic structure code with a classical trajectory package such as Venus.[214] Code for calculating the classical trajectories has also been incorporated into a number of widely distributed electronic structure packages (Dalton, DMol, Gamess, Gaussian, HyperChem, NWChem, etc.). Velocity Verlet, fourth-order Runge–Kutta, sixth-order Adams–Moulton–Bashforth and related predictor corrector algorithms[215] are popular numerical methods for integrating the equations of motion. However, fairly small time steps are required so that the integration is sufficiently accurate. Conservation of the total energy is one measure that is often used to gauge the quality of a simulation. Even though Verlet methods[216] (standard, leapfrog, and velocity) are only second order, they are remarkably good at conserving the total energy over long simulations, a property shared by all symplectic integrators.[217] For accurate integrations, time steps of 0.05 to 0.5 fs are needed for typical molecules. Thus, each trajectory may require many thousands of electronic structure calculations, even for fairly fast reactions.

For quite a number of electronic structure methods, second derivatives of the energy (Hessians) can be calculated analytically, providing a local quadratic approximation to the potential energy surface. The equations of motion can be integrated on this local surface for significantly larger steps before the electronic structure has to be recalculated. Helgaker, Uggerud, and Jensen used this approach to compute classical trajectories for H_2 + H and for $CH_2OH \rightarrow HCO^+ + H_2$ using multiconfiguration SCF calculations.[218,219] Since these initial applications, a growing number of systems have been studied by these authors with this second-order Hessian-based trajectory integration method.[220–226]

In recent work, we have developed a more accurate predictor-corrector integration algorithm that uses Hessians.[186–188] As shown in Figure 8, this scheme employs the second-order Hessian-based method as a predictor step. The Hessian is recalculated and a fifth-order polynomial is fitted to the energies, gradients, and Hessians at the beginning and end points of the predictor step. The Bulrisch–Stoer algorithm[215] is then used to reintegrate the trajectory on the fitted surface to yield a corrector step. The electronic structure work is the same as for the second-order Hessian-based method, because the energy, gradient, and Hessian at the end of the current predictor step are used for the start of the next predictor step. The error in the conservation of energy for this Hessian-based predictor corrector method is three orders of magnitude lower than for the second-order Hessian-based method, allowing for an order of magnitude increase in step size without loss of accuracy in the energy conservation (see Fig. 9).

The quasi-Newton geometry optimization algorithms described above make effective use of updating formulas to improve an estimated Hessian during the course of an optimization. The same approach can be applied to the Hessian based predictor-corrector method for integrating trajectories. Bofill's update,[95] eq. (12), was found to be the most satisfactory. The Hessian can be updated for 5–10 steps before it needs to be recalculated. Slightly smaller step sizes are needed to maintain the same energy conservation. For systems containing four to six heavy atoms this speeds up the trajectory integration by a factor of 3 or more. The Hessian-based predictor-corrector method (with and without updating) has been used in studies $H_2CO \rightarrow H_2 + CO$, $F + C_2H_4 \rightarrow C_2H_3F$, $C_2H_2O_2$

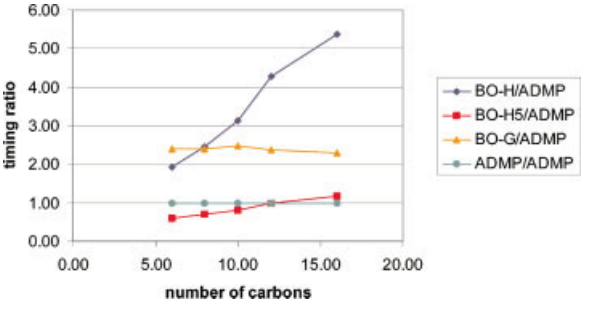

Figure 10. Ratios of estimated timings for Born–Oppenheimer vs. ADMP trajectory calculations on linear hydrocarbons, C_nH_{2n+2}, computed at the HF/6-31G(d) level of theory [second-order Hessian method (blue, diamonds), Hessian-based predictor-corrector (red, squares), gradient based velocity Verlet (orange, triangles) vs. ADMP (green, diamonds)].

(glyoxal) $\rightarrow H_2 + 2$ CO, and H_2CO + CO, $C_2N_4H_2$ (s-tetrazine) $\rightarrow N_2 + 2$ HCN and HCXO $\rightarrow$ HX + CO.[186,227–236]

Collins has developed a novel and efficient approach to direct Born–Oppenheimer dynamics.[237–242] A portion of the potential energy surface along the reaction path is mapped out with a modest number of energy, gradient, and Hessian calculations. These local quadratic patches are linked with a distance weighted interpolant to yield a global surface.

$$\begin{aligned} E(\mathbf{x}) &= \sum w_i(\mathbf{x}) T_i(\mathbf{x}), \\ w_i(\mathbf{x}) &= \nu_i(\mathbf{x}) / \sum \nu_j(\mathbf{x}), \\ \nu_i(\mathbf{x}) &= [(\|(\mathbf{x}-\mathbf{x}_i)\|/r_i)^q + (\|(\mathbf{x}-\mathbf{x}_i)\|/r_i)^p]^{-1} \\ T_i(\mathbf{x}) &= E(\mathbf{x}_i) + dE/d\mathbf{x}|_i(\mathbf{x}-\mathbf{x}_i) + \frac{1}{2}(\mathbf{x}-\mathbf{x}_i)^T d^2E/d\mathbf{x}^2|_i(\mathbf{x}-\mathbf{x}_i) \end{aligned} \tag{16}$$

where the w_i are the weights for the data points and T_i are the local Taylor expansions of the energy surface at the data points (confidence radii r_i and exponents $q << p$ control the smoothness of the interpolated surface). A set of test trajectories is run on this approximate surface. Some of these trajectories explore regions of the surface with higher uncertainty, i.e., regions farther away from the existing data points. Additional electronic structure calculations are performed in these regions to improve the accuracy of the interpolated surface. A new set of test trajectories is run and the process is repeated until the desired dynamical properties become stable with respect to improvements in the surface. This approach has been used these authors to study a number of small molecules.[243–249]

Car–Parrinello Methods

In 1985, Car and Parrinello[213] outlined a new approach to ab initio molecular dynamics (for reviews, see refs. 250–252). Rather than computing converged wavefunctions for every time step in a trajectory calculation, they decided to propagate the wavefunction. Instead of using the time-dependent Schrödinger equation (which would have necessitated very small time steps), they used an extended Lagrangian to obtain classical-like equations of motion for the wave function. Specifically, the Car–Parrinello method uses density functional theory and propagates the coefficients of the Kohn–Sham orbitals ϕ_i expanded in a plane wave basis,[253,254]

$$\mathcal{L} = \frac{1}{2}\mathrm{Tr}[\mathbf{V}^T\mathbf{M}\mathbf{V}] + \mu \sum \int |\partial\phi_i/\partial t|^2 d\mathbf{r} - E(\mathbf{R}, \phi_i) - \sum \Lambda_{ij}\left(\int \phi_i^*\phi_j d\mathbf{r} - \delta_{ij}\right) \tag{17}$$

where **R**, **V**, and **M** are the nuclear positions, velocities, and masses; μ is the fictitious electronic mass; **r** are the electronic coordinates; and Λ_{ij} are Lagrangian multipliers to ensure the orbitals remain orthonormal. The choice of a plane wave basis facilitates applications to condensed matter by building in periodic boundary conditions. This also simplifies many of the integrals; in particular, only the Hellmann–Feynman terms are needed to calculate the integrals because the basis functions do not depend on the positions of the nuclei. However, the types of density functionals that can be used easily is limited (e.g., no hybrid functionals because the Hartree–Fock exchange is difficult to calculate). To reduce the size of the plane wave basis needed, core electrons are replaced by pseudopotentials. The extended Lagrangian requires a fictitious mass, μ, for the electronic degrees of freedom. This is chosen small enough so that there is little or no exchange of energy between the nuclear and electronic degrees of freedom (if necessary, this can be controlled with thermostats). However, the fictitious mass must be chosen large enough so that the dynamics (nuclear and wavefunction) can be integrated with large enough time steps (otherwise the advantage of propagating rather than converging is lost). This approach and its variants have seen extensive usage in the physics community.[255] An alternative approach also employs a plane wave basis and pseudopotentials, but uses a conjugate gradient method to converge the wave function.[251] This is, in fact, a Born–Oppenheimer method and has some advantages over the Car–Parrinello approach in cases where the fictitious wave function dynamics run into difficulties.

Molecular electronic structure calculations in chemistry are usually carried out with atom centered basis functions (e.g., Gaussians) rather than plane waves.[3–6] For a given accuracy for an isolated molecule, far fewer atom centered functions are needed than plane waves, because they are automatically positioned where the density is the greatest. Because the density matrix becomes sparse for large molecules, Hartree–Fock and density functional calculations can be made to scale linearly with molecular size.[117,256,257] These features, along with the extensive experience that the chemistry community has with levels of theory and basis sets, lead us to develop the atom-centered density matrix propagation (ADMP) method for molecular dynamics.[258–260] In the spirit of the Car–Parrinello method, the electronic structure is propagated. Specifically, the elements of the one particle density matrix in a Gaussian basis are propagated using an extended Lagrangian.

Like density matrix search methods for calculating electronic energies,[118] the equations for propagation of the density matrix are simplest in an orthonormal basis (e.g., Löwdin or Cholesky orthonormalization). In our approach we write an extended Lagrangian for the system as

$$\mathcal{L} = \frac{1}{2}\mathrm{Tr}[\mathbf{V}^T\mathbf{M}\mathbf{V}] + \tfrac{1}{2}\mathrm{Tr}[(\mathbf{u}^{1/4}\mathbf{W}\mathbf{u}^{1/4})^2] - E(\mathbf{R}, \mathbf{P}) - \mathrm{Tr}[\mathbf{\Lambda}(\mathbf{P}\mathbf{P} - \mathbf{P})] \tag{18}$$

where **P**, **W,** and $\boldsymbol{\mu}$ are the density matrix, the density matrix velocity, and the fictitious mass matrix for the electronic degrees of freedom. Constraints on the total number of electrons and the idempotency are imposed using the Lagrangian multiplier matrix $\mathbf{\Lambda}$. The energy is calculated using the McWeeny purification of the density,[261] $\tilde{\mathbf{P}} = 3\,\mathbf{P}^2 - 2\,\mathbf{P}$.[3] The Euler–Lagrange equations of motion are:

$$\mathbf{M}d^2\mathbf{R}/dt^2 = -\partial E/\partial \mathbf{R}|_{\mathbf{P}};$$

$$d^2\mathbf{P}/dt^2 = -\mu^{-1/2}\partial E/\partial \mathbf{P}|_{\mathbf{R}} + \mathbf{\Lambda P} + \mathbf{P\Lambda} - \mathbf{\Lambda}\mu^{-1/2} \quad (19)$$

These can be integrated using the velocity Verlet algorithm,[216,253] along with a simple iterative scheme to determine the Lagrangian multipliers so that $\mathbf{P}_{i+1}$ and $\mathbf{W}_{i+1}$ satisfy the idempotency constraints.[258] In calculating $\partial E/\partial \mathbf{R}|_{\mathbf{P}}$ we need to take into account that $\mathbf{P}$ is not converged and that the transformation between the nonorthogonal atomic orbital basis and the orthonormal basis depends on $\mathbf{R}$. This leads to a somewhat more complicated expression than used for gradients of converged SCF energies. An important factor in the viability of this approach is that we have been able to obtain the derivative of the transformation matrix in closed form for both Löwdin and Cholesky orthonormalization.[258] Unlike earlier approaches to propagating Hartree–Fock and generalized valence bond wavefunctions.[262–265] the ADMP method shows excellent energy conservation without thermostats and does not require periodic reconvergence of the electronic structure.

To obtain a feel for the relative timing of the BO and ADMP methods for molecular dynamics, we considered a series of linear hydrocarbons (see Fig. 10). ADMP requires one Fock matrix and one gradient evaluation per time step, and is used as the reference. BO with velocity Verlet uses approximately the same time step but needs an average of 10 Fock matrix evaluations to converge the wave function. The Hessian-based trajectory integration methods can employ much larger time steps and still maintain the same level of energy conservation or better. When updating is used, the cost of calculating the Hessian is spread out over a number of steps. As seen in Figure 10, this approach is most efficient for small molecules and for cases that require more accurate dynamics. The ADMP approach wins for larger systems and shows its advantage even earlier for hybrid DFT methods.[260]

Some of the specific advantages of the ADMP method include the ability to treat all electrons and to employ any density functional (including hybrid functionals), the use of smaller fictitious masses and good adiabaticity without thermostats.[258–260] For ionic systems, vibrational frequencies calculated by the plane-wave Car–Parrinello method show a disturbing dependence on the fictitious electronic mass;[266] however, the ADMP method is free from this problem.[260] The ADMP trajectories compare very well with those computed by Born–Oppenheimer methods.[258] For $CH_2O \rightarrow H_2 + CO$ and $C_2H_2O_2 \rightarrow H_2 + 2\ CO$, the ADMP trajectories give product translational, rotational, and vibrational that are very close to the Born–Oppenheimer results.[260]

Summary

The capabilities of computational chemistry have expanded rapidly over the last 3–4 decades, as hardware has become orders of magnitude more powerful and software has become more efficient and sophisticated. Early calculations assumed standard geometries. As gradient methods were developed, geometry optimization became the norm. Analytic Hessians permitted easy calculation of vibrational frequencies. Algorithms for reaction path following became more sophisticated. Within the last several years, as cheap and powerful PCs have entered the market, *ab initio* molecular dynamics has become practical. The available levels of theory for these calculations have also improved during this period, from small basis set Hartree–Fock, to large correlated wave funtions and density functional methods, from one and two heavy atom molecules to systems containing thousands of atoms. The tools for exploring potential energy surfaces and the levels of theory that can be employed continue to be improved, expanding the aspects of chemistry that can be studied by electronic structure methods.

Acknowledgments

Our contributions to the exploration of potential energy surface were supported by the National Science Foundation, Wayne State University, and Gaussian, Inc. Over the years, numerous graduate students and postdoctoral fellows have been in the group: S. Anand, J. Andrés, P. Y. Ayala, A. G. Baboul, V. Bakken, W. Chen, J. B. Cross, C. L. Darling, Ö. Farkas, G. L. Fox, C. Gonzalez, M. D. Halls, H. P. Hratchian, E. W. Ignacio, J. E. Knox, J. Li, X. Li, X. Ma, F. N. Martinez, J. J. W. McDouall, J. M. Millam, I. Mincheva, C. Y. Peng, S. M. Smith, C. P. Sosa, M. D. Su, G. Tonachini, and J. M. Wittbrodt. I am also very gratefully for the many collaborations in the last 2 decades: R. D. Bach, F. Bernardi, J. F. Endicott, J. S. Francisco, M. J. Frisch, S. J. Harris, W. L. Hase, S. S. Iyengar, K. N. Kudin, R. J. Levis, S. Mobashery, K. Morokuma, M. Newcomb, J. A. Pople, M. A. Robb, G. E. Scuseria, S. Shaik, A. Skancke, P. N. Skancke, G. A. Voth, T. Vreven, P. G. Wang, C. H. Winter, and S. Wolfe. I would also like to thank the reviewers for their numerous and helpful suggestions.

References

1. Tools for Exploring Potential Energy Surfaces; in 223rd National Meeting of the American Chemical Society, Orlando, FL, 2002.
2. Frisch, M. J.; Trucks, G. W.; Schlegel, H. B.; Scuseria, G. E.; Robb, M. A.; Cheeseman, J. R.; Montgomery, J. A.; Vreven, T.; Kudin, K. N.; Burant, J. C.; Millam, J. M.; Iyengar, S.; Tomasi, J.; Barone, V.; Mennucci, B.; Cossi, M.; Scalmani, G.; Rega, N.; Petersson, G. A.; Ehara, M.; Toyota, K.; Hada, M.; Fukuda, R.; Hasegawa, J.; Ishida, M.; Nakajima, T.; Kitao, O.; Nakai, H.; Honda, Y.; Nakatsuji, H.; Li, X.; Knox, J. E.; Hratchian, H. P.; Cross, J. B.; Adamo, C.; Jaramillo, J.; Cammi, R.; Pomelli, C.; Gomperts, R.; Stratmann, R. E.; Ochterski, J.; Ayala, P. Y.; Morokuma, K.; Salvador, P.; Dannenberg, J. J.; Zakrzewski, V. G.; Dapprich, S.; Daniels, A. D.; Strain, M. C.; Farkas, Ö.; Malick, D. K.; Rabuck, A. D.; Raghavachari, K.; Foresman, J. B.; Ortiz, J. V.; Cui, Q.; Baboul, A. G.; Clifford, S.; Cioslowski, J.; Stefanov, B. B.; Liu, G.; Liashenko, A.; Piskorz, P.; Komaromi, I.; Martin, R. L.; Fox, D. J.; Keith, T.; Al-Laham, M. A.; Peng, C. Y.; Nanayakkara, A.; Challacombe, M.; Gill, P. M. W.; Johnson, B.; Chen, W.; Wong, M. W.; Andres, J. L.; Gonzalez, C.; Head–Gordon, M.; Replogle, E. S.; Pople, J. A.; Gaussian, Inc.: Pittsburgh, PA, 2002.
3. Hehre, W. J.; Radom, L.; Schleyer, P. v. R.; Pople, J. A. Ab Initio Molecular Orbital Theory; Wiley: New York, 1986.
4. Foresman, J. B.; Frisch, A. Exploring Chemistry with Electronic Structure Methods; Gaussian Inc.: Pittsburgh, PA, 1996; 2nd ed.
5. Jensen, F. Introduction to Computational Chemistry; Wiley: Chichester, 1999.

6. Cramer, C. J. Essentials of Computational Chemistry: Theories and Models; J. Wiley: West Sussex, England, 2002.
7. Leach, A. R. Molecular Modelling: Principles and Applications; Prentice Hall: Harlow, England, 2001; 2nd ed.
8. Gao, J. In Reviews in Computational Chemistry; Lipkowitz, K. B.; Boyd, D. B., Eds.; VCH: New York, 1996; p 119, vol. 7.
9. Gao, J. In Encyclopedia of Computational Chemistry; Schleyer; P. v. R.; Allinger, N. L.; Kollman, P. A.; Clark, T.; Schaefer, H. F., III; Gasteiger, J.; Schreiner, P. R., Eds.; Wiley: Chichester, 1998; 1257, vol. 2.
10. Froese, R. D. J.; Morokuma, K. In Enclopedia of Computational Chemistry; Schleyer, P. v. R.; Allinger, N. L.; Kollman, P. A.; Clark, T.; Schaefer, H. F., III; Gasteiger, J.; Schreiner, P. R., Eds.; Wiley: Chichester, 1998; 1244, vol. 2.
11. Merz, K. M.; Stanton, R. V. In Encyclopedia of Computational Chemistry; Schleyer, P. v. R.; Allinger, N. L.; Kollman, P. A.; Clark, T.; Schaefer, H. F.; Gasteiger, J.; Schreiner, P. R., Eds.; Wiley: Chichester, 1998; 2330, vol. 4.
12. Tomasi, J.; Pomelli, C. S. In Encyclopedia of Computational Chemistry; Schleyer, P. v. R.; Allinger, N. L.; Kollman, P. A.; Clark, T.; Schaefer, H. F., III; Gasteiger, J.; Schreiner, P. R., Eds.; Wiley: Chichester, 1998; 2343, vol. 4.
13. Ruiz-López, M. F.; Rivail, J. L. In Encyclopedia of Computational Chemistry; Schleyer, P. v. R.; Allinger, N. L.; Kollman, P. A.; Clark, T.; Schaefer, H. F., III; Gasteiger, J.; Schreiner, P. R., Eds.; Wiley: Chichester, 1998; 437, vol. 1.
14. Monard, G.; Merz, K. M. Acc Chem Res 1999, 32, 904.
15. Mordasini, T. Z.; Thiel, W. Combined quantum mechanical and molecular mechanical approaches; Chimia: 1998; 52, 288.
16. Field, M. J.; Bash, P. A.; Karplus, M. J Comput Chem 1990, 11, 700.
17. Singh, U. C.; Kollman, P. A. J Comput Chem 1986, 7, 718.
18. Warshel, A.; Levitt, M. J Mol Biol 1976, 103, 227.
19. Allen, M. P.; Tildesley, D. J. Computer Simulation of Liquids; Oxford University Press: Oxford, England, 1987.
20. Haile, J. M. Molecular Dynamics Simulation: Elementary Methods; Wiley: New York, 1992.
21. Thompson, D. L. In Encyclopedia of Computational Chemistry; Schleyer, P. v. R.; Allinger, N. L.; Kollman, P. A.; Clark, T.; Schaefer, H. F., III; Gasteiger, J.; Schreiner, P. R., Eds.; Wiley: Chichester, 1998; 3056, vol. 5.
22. Hase, W. L., Ed. Advances in Classical Trajectory Methods; JAI Press: Greenwich, 1992.
23. Bunker, D. L. Methods Comput Phys 1971, 10, 287.
24. Raff, L. M.; Thompson, D. L. In Theory of Chemical Reaction Dynamics; Baer, M., Ed.; CRC Press: Boca Raton, 1985.
25. Bolton, K.; Hase, W. L.; Peslherbe, G. H. In Modern Methods for Multidimensional Dynamics Computation in Chemistry; Thompson, D. L., Ed.; World Scientific: Singapore, 1998; p 143.
26. Schlegel, H. B. In Modern Electronic Structure Theory; Yarkony, D. R., Ed.; World Scientific Publishing: Singapore, 1995, p. 459.
27. Schlegel, H. B. In Encyclopedia of Computational Chemistry; Schleyer, P. v. R.; Allinger, N. L.; Kollman, P. A.; Clark, T.; Schaefer, H. F., III; Gasteiger, J.; Schreiner, P. R., Eds.; Wiley: Chichester, 1998; 1136, vol. 2.
28. Schlick, T. In Encyclopedia of Computational Chemistry; Schleyer, P. v. R.; Allinger, N. L.; Kollman, P. A.; Clark, T.; Schaefer, H. F., III; Gasteiger, J.; Schreiner, P. R., Eds.; Wiley: Chichester, 1998; 1142, vol. 2.
29. Jensen, F. In Encyclopedia of Computational Chemistry; Schleyer, P. v. R.; Allinger, N. L.; Kollman, P. A.; Clark, T.; Schaefer, H. F., III; Gasteiger, J.; Schreiner, P. R., Eds.; Wiley: Chichester, 1998; p 3114, vol. 5.
30. Wales, D. J. Energy Landscapes; Cambridge University Press: Cambridge, 2003.
31. Farkas, Ö.; Schlegel, H. B. J Chem Phys 1998, 109, 7100.
32. Farkas, Ö.; Schlegel, H. B. J Chem Phys 1999, 111, 10806.
33. Farkas, Ö.; Schlegel, H. B. Phys Chem Chem Phys 2002, 4, 11.
34. Paizs, B.; Fogarasi, G.; Pulay, P. J Chem Phys 1998, 109, 6571.
35. Paizs, B.; Baker, J.; Suhai, S.; Pulay, P. J Chem Phys 2000, 113, 6566.
36. Nemeth, K.; Coulaud, O.; Monard, G.; Angyan, J. G. J Chem Phys 2000, 113, 5598.
37. Nemeth, K.; Coulaud, O.; Monard, G.; Angyan, J. G. J Chem Phys 2001, 114, 9747.
38. Billeter, S. R.; Turner, A. J.; Thiel, W. Phys Chem Chem Phys 2000, 2, 2177.
39. Baker, J.; Kinghorn, D.; Pulay, P. J Chem Phys 1999, 110, 4986.
40. Zhang, Y. K.; Liu, H. Y.; Yang, W. T. J Chem Phys 2000, 112, 3483.
41. Sierka, M.; Sauer, J. J Chem Phys 2000, 112, 6983.
42. Turner, A. J.; Moliner, V.; Williams, I. H. Phys Chem Chem Phys 1999, 1, 1323.
43. Vreven, T.; Morokuma, K.; Farkas, Ö.; Schlegel, H. B.; Frisch, M. J. J Comput Chem 2003, to appear.
44. Head–Gordon, M.; Pople, J. A. J Phys Chem 1988, 92, 3063.
45. Head–Gordon, M.; Pople, J. A.; Frisch, M. J. Int J Quantum Chem 1989, 291.
46. Fischer, T. H.; Almlof, J. J Phys Chem 1992, 96, 9768.
47. Li, X.; Schlegel, H. B., in preparation.
48. Floudas, C. A.; Pardalos, P. M. Optimization in Computational Chemistry and Molecular Biology: Local and Global Approaches; Kluwer Academic Publishers: Dordrecht, 2000.
49. Horst, R.; Pardalos, P. M. Handbook of Global Optimization; Kluwer Academic Publishers: Dordrecht, 1995.
50. Horst, R.; Pardalos, P. M.; Thoai, N. V. Introduction to Global Optimization; Kluwer Academic Publishers: Dordrecht, 2000, 2nd ed.
51. Törn, A.; Zhilinskas, A. Global Optimization; Springer-Verlag: Berlin, 1989.
52. Floudas, C. A.; Pardalos, P. M. State of the Art in Global Optimization: Computational Methods and Applications; Kluwer Academic Publishers: Dordrecht, 1996.
53. Schlegel, H. B. In Encyclopedia of Computational Chemistry; Schleyer, P. v. R.; Allinger, N. L.; Kollman, P. A.; Clark, T.; Schaefer, H. F., III; Gasteiger, J.; Schreiner, P. R., Eds.; Wiley: Chichester, 1998; p 2432, vol. 4.
54. Heidrich, D. The Reaction Path in Chemistry: Current Approaches and Perspectives; Kluwer: Dordrecht, 1995.
55. Collins, M. A. Adv Chem Phys 1996, 93, 389.
56. McKee, M. L.; Page, M. In Reviews in Computational Chemistry; Lipkowitz, K. B.; Boyd, D. B., Eds.; VCH: New York, 1993; p 35, vol. 4.
57. Elber, R.; Karplus, M. Chem Phys Lett 1987, 139, 375.
58. Czerminski, R.; Elber, R. Int J Quantum Chem 1990, Suppl. 24, 167.
59. Ulitsky, A.; Elber, R. J Chem Phys 1990, 92, 1510.
60. Henkelman, G.; Jonsson, H. J Chem Phys 2000, 113, 9978.
61. Maragakis, P.; Andreev, S. A.; Brumer, Y.; Reichman, D. R.; Kaxiras, E. J Chem Phys 2002, 117, 4651.
62. Ayala, P. Y.; Schlegel, H. B. J Chem Phys 1997, 107, 375.
63. Choi, C.; Elber, R. J Chem Phys 1991, 94, 751.
64. Fischer, S.; Karplus, M. Chem Phys Lett 1992, 194, 252.
65. Stewart, J. J. P.; Davis, L. P.; Burggraf, L. W. J Comput Chem 1987, 8, 1117.
66. Maluendes, S. A.; Dupuis, M. J Chem Phys 1990, 93, 5902.
67. Gordon, M. S.; Chaban, G.; Taketsugu, T. J Phys Chem 1996, 100, 11512.

68. Hratchian, H. P.; Schlegel, H. B. J Phys Chem A 2002, 106, 165.
69. Liotard, D. A. Int J Quantum Chem 1992, 44, 723.
70. Truhlar, D. G.; Garrett, B. C. Annu Rev Phys Chem 1984, 35, 159.
71. Truhlar, D. G.; Garrett, B. C.; Klippenstein, S. J. J Phys Chem 1996, 100, 12771.
72. Garrett, B. C.; Truhlar, D. G. In Encyclopedia of Computational Chemistry; Schleyer, P. v. R.; Allinger, N. L.; Kollman, P. A.; Clark, T.; Schaefer, H. F., III; Gasteiger, J.; Schreiner, P. R., Eds.; Wiley: Chichester, 1998; 3094, vol. 2.
73. Miller, W. H.; Handy, N. C.; Adams, J. E. J Chem Phys 1980, 72, 99.
74. Kraka, E. In Encyclopedia of Computational Chemistry; Schleyer, P. v. R.; Allinger, N. L.; Kollman, P. A.; Clark, T.; Schaefer, H. F., III; Gasteiger, J.; Schreiner, P. R., Eds.; Wiley: Chichester, 1998; p 2437, vol. 2.
75. Ben–Nun, M.; Martinez, T. J. Adv Chem Phys 2002, 121, 439.
76. Voth, G. A. J Phys Chem A 1999, 103, 9383.
77. Kosloff, R. Annu Rev Phys Chem 1994, 45, 145.
78. Pulay, P.; Fogarasi, G. J Chem Phys 1992, 96, 2856.
79. Fogarasi, G.; Zhou, X. F.; Taylor, P. W.; Pulay, P. J Am Chem Soc 1992, 114, 8191.
80. Baker, J.; Kessi, A.; Delley, B. J Chem Phys 1996, 105, 192.
81. Peng, C. Y.; Ayala, P. Y.; Schlegel, H. B.; Frisch, M. J. J Comput Chem 1996, 17, 49.
82. von Arnim, M.; Ahlrichs, R. J Chem Phys 1999, 111, 9183.
83. Kudin, K. N.; Scuseria, G. E.; Schlegel, H. B. J Chem Phys 2001, 114, 2919.
84. Wilson, E. B.; Decius, J. C.; Cross, P. C. Molecular Vibrations: The Theory of Infrared and Raman Vibrational Spectra; Dover Publications: New York, 1980.
85. Fletcher, R. Practical Methods of Optimization; Wiley: Chichester, 1987; 2nd ed.
86. Dennis, J. E.; Schnabel, R. B. Numerical Methods for Unconstrained Optimization and Nonlinear Equations; Prentice-Hall: Englewood Cliffs, NJ, 1983.
87. Scales, L. E. Introduction to Non-Linear Optimization; Springer-Verlag: New York, 1985.
88. Gill, P. E.; Murray, W.; Wright, M. H. Practical Optimization; Academic Press: London, 1981.
89. Schlegel, H. B. Theor Chim Acta 1984, 66, 333.
90. Wittbrodt, J. M.; Schlegel, H. B. Theochem J Mol Struct 1997, 398, 55.
91. Broyden, C. G. J Inst Math Appl 1970, 6, 76.
92. Fletcher, R. Comput J 1970, 13, 317.
93. Goldfarb, D. Math Comput 1970, 24, 23.
94. Shanno, D. F. Math Comput 1970, 24, 647.
95. Bofill, J. M. J Comput Chem 1994, 15, 1.
96. Morales, J. L.; Nocedal, J. SIAM J Optim 2000, 10, 1079.
97. Byrd, R. H.; Lu, P. H.; Nocedal, J.; Zhu, C. Y. SIAM J Sci Comput 1995, 16, 1190.
98. Biegler, L. T.; Nocedal, J.; Schmid, C. SIAM J Optim 1995, 5, 314.
99. Fletcher, R. SIAM J Optim 1995, 5, 192.
100. Byrd, R. H.; Nocedal, J.; Schnabel, R. B. Math Program 1994, 63, 129.
101. Liu, D. C.; Nocedal, J. Math Program 1989, 45, 503.
102. Nocedal, J. Math Comput 1980, 35, 773.
103. Anglada, J. M.; Besalu, E.; Bofill, J. M.; Rubio, J. J Math Chem 1999, 25, 85.
104. Prat-Resina, X.; Garcia–Viloca, M.; Monard, G.; Gonzalez–Lafont, A.; Lluch, J. M.; Bofill, J. M.; Anglada, J. M. Theor Chem Acc 2002, 107, 147.
105. Banerjee, A.; Adams, N.; Simons, J.; Shepard, R. J Phys Chem 1985, 89, 52.
106. Helgaker, T. Chem Phys Lett 1991, 182, 503.
107. Culot, P.; Dive, G.; Nguyen, V. H.; Ghuysen, J. M. Theor Chim Acta 1992, 82, 189.
108. Anglada, J. M.; Bofill, J. M. Int J Quantum Chem 1997, 62, 153.
109. Besalu, E.; Bofill, J. M. Theor Chem Acc 1998, 100, 265.
110. Schlegel, H. B. J Comput Chem 1982, 3, 214.
111. Csaszar, P.; Pulay, P. J Mol Struct 1984, 114, 31.
112. Farkas, Ö. PhD (Csc) thesis; Eötvös Loránd University and Hungarian Academy of Sciences: Budapest, 1995.
113. Svensson, M.; Humbel, S.; Froese, R. D. J.; Matsubara, T.; Sieber, S.; Morokuma, K. J Phys Chem 1996, 100, 19357.
114. Dapprich, S.; Komaromi, I.; Byun, K. S.; Morokuma, K.; Frisch, M. J. Theochem J Mol Struct 1999, 462, 1.
115. Vreven, T.; Mennucci, B.; da Silva, C. O.; Morokuma, K.; Tomasi, J. J Chem Phys 2001, 115, 62.
116. Bacskay, G. B. Chem Phys 1981, 61, 385.
117. Li, X. P.; Nunes, W.; Vanderbilt, D. Phys Rev B 1993, 47, 10891.
118. Millam, J. M.; Scuseria, G. E. J Chem Phys 1997, 106, 5569.
119. Cances, E.; Le Bris, C. ESAIM-Math Model Numer Anal Model Math Anal Numer 2000, 34, 749.
120. Larsen, H.; Olsen, J.; Jorgensen, P.; Helgaker, T. J Chem Phys 2001, 115, 9685.
121. Kudin, K. N.; Scuseria, G. E.; Cances, E. J Chem Phys 2002, 116, 8255.
122. Van Voorhis, T.; Head–Gordon, M. Mol Phys 2002, 100, 1713.
123. Schlegel, H. B., unpublished.
124. Yarkony, D. R. J Phys Chem A 2001, 105, 6277.
125. Yarkony, D. R. Acc Chem Res 1998, 31, 511.
126. Yarkony, D. R. Rev Mod Phys 1996, 68, 985.
127. Yarkony, D. R. J Chem Phys 1990, 92, 2457.
128. Yarkony, D. R. J Phys Chem 1993, 97, 4407.
129. Anglada, J. M.; Bofill, J. M. J Comput Chem 1997, 18, 992.
130. Bearpark, M. J.; Robb, M. A.; Schlegel, H. B. Chem Phys Lett 1994, 223, 269.
131. Poppinger, D. Chem Phys Lett 1975, 35, 550.
132. McIver, J. W.; Komornicki, A. J Am Chem Soc 1972, 94, 2625.
133. Komornicki, A.; Ishida, K.; Morokuma, K.; Ditchfield, R.; Conrad, M. Chem Phys Lett 1977, 45, 595.
134. Kliesch, W.; Schenk, K.; Heidrich, D.; Dachsel, H. J Comput Chem 1988, 9, 810.
135. Bofill, J. M.; Comajuan, M. J Comput Chem 1995, 16, 1326.
136. Bofill, J. M. Chem Phys Lett 1996, 260, 359.
137. Anglada, J. M.; Bofill, J. M. J Comput Chem 1998, 19, 349.
138. Bofill, J. M.; Anglada, J. M. Theor Chem Acc 2001, 105, 463.
139. Anglada, J. M.; Besalu, E.; Bofill, J. M.; Crehuet, R. J Comput Chem 2001, 22, 387.
140. McDouall, J. J. W.; Robb, M. A.; Bernardi, F. Chem Phys Lett 1986, 129, 595.
141. Bernardi, F.; McDouall, J. J. W.; Robb, M. A. J Comput Chem 1987, 8, 296.
142. Jensen, F. J Comput Chem 1994, 15, 1199.
143. Anglada, J. M.; Besalu, E.; Bofill, J. M.; Crehuet, R. J Comput Chem 1999, 20, 1112.
144. Williams, I. H.; Maggiora, G. M. Theochem J Mol Struct 1982, 6, 365.
145. Scharfenberg, P. Chem Phys Lett 1981, 79, 115.
146. Rothman, M. J.; Lohr, L. L. Chem Phys Lett 1980, 70, 405.
147 Quapp, W. Chem Phys Lett 1996, 253, 286.
148. Quapp, W.; Hirsch, M.; Imig, O.; Heidrich, D. J Comput Chem 1998, 19, 1087.
149. Quapp, W.; Hirsch, M.; Heidrich, D. Theor Chem Acc 2000, 105, 145.
150. Quapp, W. Searching minima of an n-dimensional surface: A robust valley following method. Comput Math Appl 2001, 41, 407.

151. Hirsch, M.; Quapp, W. J Comput Chem 2002, 23, 887.
152. Crehuet, R.; Bofill, J. M.; Anglada, J. M. Theor Chem Acc 2002, 107, 130.
153. Cerjan, C. J.; Miller, W. H. J Chem Phys 1981, 75, 2800.
154. Simons, J.; Jorgensen, P.; Taylor, H.; Ozment, J. J Phys Chem 1983, 87, 2745.
155. Simons, J.; Nichols, J. Int J Quantum Chem 1990, Suppl. 24, 263.
156. Nichols, J.; Taylor, H.; Schmidt, P.; Simons, J. J Chem Phys 1990, 92, 340.
157. Baker, J. J Comput Chem 1986, 7, 385.
158. Pancir, J. Collect Czech Chem Commun 1975, 40, 1112.
159. Basilevsky, M. V.; Shamov, A. G. Chem Phys 1981, 60, 347.
160. Hoffman, D. K.; Nord, R. S.; Ruedenberg, K. Theor Chim Acta 1986, 69, 265.
161. Jorgensen, P.; Jensen, H. J. A.; Helgaker, T. Theor Chim Acta 1988, 73, 55.
162. Schlegel, H. B. Theor Chim Acta 1992, 83, 15.
163. Sun, J. Q.; Ruedenberg, K. J Chem Phys 1993, 98, 9707.
164. Bondensgård, K.; Jensen, F. J Chem Phys 1996, 104, 8025.
165. Halgren, T.; Lipscomb, W. N. Chem Phys Lett 1977, 49, 225.
166. Peng, C. Y.; Schlegel, H. B. Isr J Chem 1993, 33, 449.
167. Mueller, K.; Brown, L. D. Theor Chim Acta 1979, 53, 75.
168. Dewar, M. J. S.; Healy, E. F.; Stewart, J. J. P. J Chem Soc Faraday Trans II 1984, 80, 227.
169. Cardenas–Lailhacar, C.; Zerner, M. C. Int J Quantum Chem 1995, 55, 429.
170. Ionova, I. V.; Carter, E. A. J Chem Phys 1993, 98, 6377.
171. Ionova, I. V.; Carter, E. A. J Chem Phys 1995, 103, 5437.
172. Irikura, K. K.; Johnson, R. D. J Phys Chem A 2000, 104, 2191.
173. Cernohorsky, M.; Kettou, S.; Koca, J. J Chem Inf Comput Sci 1999, 39, 705.
174. Muller, E. M.; de Meijere, A.; Grubmuller, H. J Chem Phys 2002, 116, 897.
175. Fukui, K. Acc Chem Res 1981, 14, 363.
176. Ishida, K.; Morokuma, K.; Komornicki, A. J Chem Phys 1977, 66, 2153.
177. Page, M.; McIver, J. W. J Chem Phys 1988, 88, 922.
178. Page, M.; Doubleday, C.; McIver, J. W. J Chem Phys 1990, 93, 5634.
179. Garrett, B. C.; Redmon, M. J.; Steckler, R.; Truhlar, D. G.; Baldridge, K. K.; Bartol, D.; Schmidt, M. W.; Gordon, M. S. J Phys Chem 1988, 92, 1476.
180. Baldridge, K. K.; Gordon, M. S.; Steckler, R.; Truhlar, D. G. J Phys Chem 1989, 93, 5107.
181. Melissas, V. S.; Truhlar, D. G.; Garrett, B. C. J Chem Phys 1992, 96, 5758.
182. Gear, C. W. Numerical Initial Value Problems in Ordinary Differential Equations; Prentice-Hall: Englewood Cliffs, NJ, 1971.
183. Gonzalez, C.; Schlegel, H. B. J Chem Phys 1989, 90, 2154.
184. Gonzalez, C.; Schlegel, H. B. J Phys Chem 1990, 94, 5523.
185. Gonzalez, C.; Schlegel, H. B. J Chem Phys 1991, 95, 5853.
186. Chen, W.; Hase, W. L.; Schlegel, H. B. Chem Phys Lett 1994, 228, 436.
187. Millam, J. M.; Bakken, V.; Chen, W.; Hase, W. L.; Schlegel, H. B. J Chem Phys 1999, 111, 3800.
188. Bakken, V.; Millam, J. M.; Schlegel, H. B. J Chem Phys 1999, 111, 8773.
189. Baboul, A. G.; Schlegel, H. B. J Chem Phys 1997, 107, 9413.
190. Brooks, B. R.; Lee, Y. S.; Cheatham, T. E. Abstr Pap Am Chem Soc 2001, 222, 63-COMP.
191. Michalak, A.; Ziegler, T. J Phys Chem A 2001, 105, 4333.
192. Crooks, G. E.; Chandler, D. Phys Rev E 2001, 6402, 026109.
193. Bolhuis, P. G.; Dellago, C.; Geissler, P. L.; Chandler, D. J Phys Condes Matter 2000, 12, A147.
194. Dellago, C.; Bolhuis, P. G.; Chandler, D. J Chem Phys 1999, 110, 6617.
195. Bolhuis, P. G.; Dellago, C.; Chandler, D. Faraday Discuss 1998, 421.
196. Dellago, C.; Bolhuis, P. G.; Csajka, F. S.; Chandler, D. J Chem Phys 1998, 108, 1964.
197. Rosso, L.; Tuckerman, M. E. Mol Simul 2002, 28, 91.
198. Rosso, L.; Minary, P.; Zhu, Z. W.; Tuckerman, M. E. J Chem Phys 2002, 116, 4389.
199. Schatz, G. C. Rev Mod Phys 1989, 61, 669.
200. Schatz, G. C. In Advances in Molecular Electronic Structure Theory; Dunning, T. H., Ed.; JAI Press: London, 1990.
201. Hase, W. L. In Encyclopedia of Computational Chemistry; Schleyer, P. v. R.; Allinger, N. L.; Clark, T.; Gasteiger, J.; Kollman, P. A.; Scheafer, H. F., III; Schreiner, P. R., Eds.; Wiley: Chichester, 1998; p 402.
202. Hase, W. L. In Encyclopedia of Computational Chemistry; Schleyer, P. v. R.; Allinger, N. L.; Clark, T.; Gasteiger, J.; Kollman, P. A.; Scheafer, H. F., III; Schreiner, P. R., Eds.; Wiley: Chichester, 1998; p 399.
203. Rapaport, D. C. The Art of Molecular Dynamics Simulation; Cambridge University Press: Cambridge, 1995.
204. Frenkel, D.; Smit, B. Understanding Molecular Simulation: from Algorithms to Applications; Academic Press: San Diego, 2002; 2nd ed.
205. McCammon, J. A.; Harvey, S. C. Dynamics of Proteins and Nucleic Acids; Cambridge University Press: Cambridge, 1987.
206. Gunsteren, W. F. v.; Weiner, P. K.; Wilkinson, A. J. Computer Simulation of Biomolecular Systems: Theoretical and Experimental Applications; ESCOM: Leiden, 1989.
207. Kollman, P. Chem Rev 1993, 93, 2395.
208. Beveridge, D. L.; Dicapua, F. M. Annu Rev Biophys Biophys Chem 1989, 18, 431.
209. Beveridge, D. L. In Encyclopedia of Computational Chemistry; Schleyer, P. v. R.; Allinger, N. L.; Kollman, P. A.; Clark, T.; Schaefer, H. F., III; Gasteiger, J.; Schreiner, P. R., Eds.; Wiley: Chichester, 1998, 0.1620, vol. 3.
210. Auffinger, P.; Weshof, E. In Encyclopedia of Computational Chemistry; Schleyer, P. v. R.; Allinger, N. L.; Kollman, P. A.; Clark, T.; Schaefer, H. F., III; Gasteiger, J.; Schreiner, P. R., Eds.; Wiley: Chichester, 1998, p. 1628, vol. 3.
211. Berendsen, H. J. C.; Tieleman, D. P. In Encyclopedia of Computational Chemistry; Schleyer, P. v. R.; Allinger, N. L.; Kollman, P. A.; Clark, T.; Schaefer, H. F., III; Gasteiger, J.; Schreiner, P. R., Eds.; Wiley: Chichester, 1998, p. 1639, vol. 3.
212. Pedersen, L.; Darden, T. In Encyclopedia of Computational Chemistry; Schleyer, P. v. R.; Allinger, N. L.; Kollman, P. A.; Clark, T.; Schaefer, H. F., III; Gasteiger, J.; Schreiner, P. R., Eds.; Wiley: Chichester, 1998, p. 1650, vol. 3.
213. Car, R.; Parrinello, M. Phys Rev Lett 1985, 55, 2471.
214. Hase, W. L.; Duchovic, R. J.; Hu, X.; Kormonick, A.; Lim, K.; Lu, D.-H.; Peslherbe, G. H.; Swamy, K. N.; Vande Linde, S. R.; Varandas, A. J. C.; Wang, H.; Wolfe, R. J. QCPE 1996, 16, 671.
215. Press, W. H. Numerical Recipes in FORTRAN: The Art of Scientific Computing; Cambridge University Press: Cambridge, England, 1992; 2nd ed.
216. Swope, W. C.; Andersen, H. C.; Berens, P. H.; Wilson, K. R. J Chem Phys 1982, 76, 637.
217. McLachlan, R. I.; Atela, P. Nonlinearity 1992, 5, 541.
218. Helgaker, T.; Uggerud, E.; Jensen, H. J. A. Chem Phys Lett 1990, 173, 145.
219. Uggerud, E.; Helgaker, T. J Am Chem Soc 1992, 114, 4265.
220. Braten, S. M.; Helgaker, T.; Uggerud, E. Org Mass Spectrom 1993, 28, 1262.

221. Bueker, H. H.; Uggerud, E. J Phys Chem 1995, 99, 5945.
222. Bueker, H. H.; Helgaker, T.; Ruud, K.; Uggerud, E. J Phys Chem 1996, 100, 15388.
223. Oiestad, A. M. L.; Uggerud, E. Int J Mass Spectrom 1997, 167, 117.
224. Oiestad, E. L.; Uggerud, E. Int J Mass Spectrom 1997, 165, 39.
225. Ruud, K.; Helgaker, T.; Uggerud, E. Theochem J Mol Struct 1997, 393, 59.
226. Uggerud, E. Mass Spectrom Rev 1999, 18, 285.
227. Vreven, T.; Bernardi, F.; Garavelli, M.; Olivucci, M.; Robb, M. A.; Schlegel, H. B. J Am Chem Soc 1997, 119, 12687.
228. Bolton, K.; Hase, W. L.; Schlegel, H. B.; Song, K. Chem Phys Lett 1998, 288, 621.
229. Bolton, K.; Schlegel, H. B.; Hase, W. L.; Song, K. Y. Phys Chem Chem Phys 1999, 1, 999.
230. Sanchez–Galvez, A.; Hunt, P.; Robb, M. A.; Olivucci, M.; Vreven, T.; Schlegel, H. B. J Am Chem Soc 2000, 122, 2911.
231. Li, X. S.; Millam, J. M.; Schlegel, H. B. J Chem Phys 2000, 113, 10062.
232. Bakken, V.; Danovich, D.; Shaik, S.; Schlegel, H. B. J Am Chem Soc 2001, 123, 130.
233. Li, X. S.; Millam, J. M.; Schlegel, H. B. J Chem Phys 2001, 114, 8897.
234. Li, X. S.; Millam, J. M.; Schlegel, H. B. J Chem Phys 2001, 115, 6907.
235. Li, X. S.; Anand, S.; Millam, J. M.; Schlegel, H. B. Phys Chem Chem Phys 2002, 4, 2554.
236. Anand, S.; Schlegel, H. B. J Phys Chem A 2002, 106, 11623.
237. Ischtwan, J.; Collins, M. J Chem Phys 1994, 100, 8080.
238. Jordan, M. J. T.; Thompson, K. C.; Collins, M. A. J Chem Phys 1995, 103, 9669.
239. Thompson, K. C.; Collins, M. A. J Chem Soc Faraday Trans 1997, 93, 871.
240. Thompson, K. C.; Jordan, M. J. T.; Collins, M. A. J Chem Phys 1998, 108, 8302.
241. Bettens, R. P. A.; Collins, M. A. J Chem Phys 1999, 111, 816.
242. Collins, M. A. Theor Chem Acc 2002, 108, 313.
243. Jordan, M. J. T.; Thompson, K. C.; Collins, M. A. J Chem Phys 1995, 102, 5647.
244. Jordan, M. J. T.; Collins, M. A. J Chem Phys 1996, 104, 4600.
245. Bettens, R. P. A.; Collins, M. A. J Chem Phys 1998, 109, 9728.
246. Bettens, R. P. A.; Hansen, T. A.; Collins, M. A. J Chem Phys 1999, 111, 6322.
247. Collins, M. A.; Zhang, D. H. J Chem Phys 1999, 111, 9924.
248. Fuller, R. O.; Bettens, R. P. A.; Collins, M. A. J Chem Phys 2001, 114, 10711.
249. Song, K. Y.; Collins, M. A. Chem Phys Lett 2001, 335, 481.
250. Remler, D. K.; Madden, P. A. Mol Phys 1990, 70, 921.
251. Payne, M. C.; Teter, M. P.; Allan, D. C.; Arias, T. A.; Joannopoulos, J. D. Rev Mod Phys 1992, 64, 1045.
252. Marx, D.; Hutter, J. In Modern Methods and Algorithms of Quantum Chemistry; Grotendorst, J., Ed.; John vonNeumann Institute for Computing: Julich, 2000; p 301, vol. 1.
253. Tuckerman, M. E.; Parrinello, M. J Chem Phys 1994, 101, 1302.
254. Tuckerman, M. E.; Parrinello, M. J Chem Phys 1994, 101, 1316.
255. Rothlisberger, U. Comput Chem 2001, 6, 33.
256. Goedecker, S. Rev Mod Phys 1999, 71, 1085.
257. Scuseria, G. E. Linear scaling density functional calculations with Gaussian orbitals. J Phys Chem A 1999, 103, 4782.
258. Schlegel, H. B.; Millam, J. M.; Iyengar, S. S.; Voth, G. A.; Daniels, A. D.; Scuseria, G. E.; Frisch, M. J. J Chem Phys 2001, 114, 9758.
259. Iyengar, S. S.; Schlegel, H. B.; Millam, J. M.; Voth, G. A.; Scuseria, G. E.; Frisch, M. J. J Chem Phys 2001, 115, 10291.
260. Schlegel, H. B.; Iyengar, S. S.; Li, X.; Millam, J. M.; Voth, G. A.; Scuseria, G. E.; Frisch, M. J. J Chem Phys 2002, 117, 8694.
261. McWeeny, R. Rev Mod Phys 1960, 32, 335.
262. Hartke, B.; Carter, E. A. J Chem Phys 1992, 97, 6569.
263. Hartke, B.; Carter, E. A. Chem Phys Lett 1992, 189, 358.
264. Gibson, D. A.; Carter, E. A. J Phys Chem 1993, 97, 13429.
265. Gibson, D. A.; Ionova, I. V.; Carter, E. A. Chem Phys Lett 1995, 240, 261.
266. Tangney, P.; Scandolo, S. J Chem Phys 2002, 116, 14.
267. Schlegel, H. B. Adv Chem Phys 1987, 67, 249.